Research Square

Preprints are preliminary reports that have not undergone peer review.
They should not be considered conclusive, used to inform clinical practice,
or referenced by the media as validated information.

Study The Effect of Nanoclays on The Mechanical Properties of Polypropylene/Polyamide66 Nanocomoposites

Benalia Kouini

kouinib@univ-boumerdes.dz

M'Hamed Bougara University

Research Article

Keywords: Nanoclay, nanocomposites, polypropylene, polyamide, melt processing, mechanical properties

Posted Date: March 31st, 2026

DOI: https://doi.org/10.21203/rs.3.rs-9253808/v1

License: This work is licensed under a Creative Commons Attribution 4.0 International License.
Read Full License

Additional Declarations: No competing interests reported.

Abstract

Nanocomposites based on polypropylene/polyamide66 (PP/PA66) nanoblends containing organophilic montmorillonite (OMMT) and maleic anhydride grafted polypropylene (PP-g-MAH) were prepared by melt compounding method followed by injection molding. Two different types of nanoclays were used in this work, i.e. DELLITE LVF (untreated): is a nano-clay deriving from a naturally occurring especially purified montmorillonite and DELLITE 67G (treated with a high content of quaternary ammonium salt (dimethyl dehydrogenated tallow ammonium). The rheological results revealed a drastic reduction in MFI with a levelling off at 5 wt.% for the nanoblends containing treated clay. The impact properties of PP/PA66 modified nanoblends were improved significantly in the presence of treated nanoclay. The morphology of the nanocomposites was studied using the XR diffraction (XRD).

XRD results revealed the formation of nanoblends as the nanoclay was intercalated and exfoliated.

1. Introduction

Polymer/organoclay nanocomposites present specific properties that are not observed in conventional composites. The achievement of compatibilization, whether by addition a compatibilizer or by in situ chemical reaction between blend components (reactive blending), has played an important role in the development of polymer blends and provide a good solution for needs of industry [1]. Engineering polymers are being increasingly used in a wide number of applications [2]. The aims behind the incorporation of small amounts of organoclay (< 10wt.%) into polymer matrices may remarkably improve dimension stability, mechanical, thermal, optical, electrical, and gas barrier properties, and decrease the flammability of polymer-polymer blends [1, 3]. It is known that blends of PP and PA66 are immiscible throughout the whole range of composition, and thus exhibit poor properties [4].

Unfavourable interactions at the molecular level lead to high interfacial tension and make the melt mixing of the components difficult. This also leads to unstable morphology and poor interfacial adhesion, which are the main causes for inferior mechanical properties of the blends [5]. In order to prevent the compatibility problem, a suitable compatibilizer is synthesised by grafting MAH onto PP (PP-g-MAH) because it has anhydride and carboxyl groups that interact with functional groups of the PA66. Numerous researchers described polymer-clay nanocomposites based on single polymer matrix [6]. However, thermoplastic nanocomposites based on blends of two or more polymeric materials, i.e.binary or ternary blends; seem to be a new approach in the nanocomposites studies. The work presented in this paper focuses on the study of thermoplastic nanocomposites based on blends of PP and PA66 and modified by nanoclay (treated and untreated).The aim of this work was to study the effect of nanoclay loading from 2 up to 8%wt on the rheological ,mechanical and morphological properties of PP-PPgMAH-PA66 nanoblends.

2. EXPRIMENTAL

2.1 Materials

Table 1 summarizes the materials used in this work as well as the specific characteristics and the suppliers.

Table 1
Materials

Materials (Trade name)	**Characteristics**	**Supplier**
Isotactic Polypropylene (MOPLEN)	- semi-crystalline polymer - MFI = 28[g/10 min],(2190 g at 230°C)	HIMONT Company
Polyamide 66 (Technyl→A216)	Was used as the dispersed (minor) phase in the blend	Rhone Poulenc Company
Untreated nanoclays (DELLITE LVF)	nanoclay deriving from a naturally occurring especially purified montmorillonite	Laviosa Company
Treated nanoclays (DELLITE 67G)	Treated with a high content of quaternary ammonium salt (dimethyl dehydrogenated tallow ammonium).	Laviosa Company

2.2. Specimen Preparation of PP/PA66/Nanoclay Nanocomposites

The first operation consists of mixing PP with 0.6%wt antioxidant and the second one concern the preparation of the modified PP with PP-g-MAH as a compatibilizer [8]. Both operations are done in a single screw extruder. The following operation concerns the preparation of modified (with nanoclay) and unmodified 70/30/5 wt % PP/PA66/PP-g-MAH nanoblends. The materials were mixed in a high shear internal batch Rheocard Haake mixer chamber. The mixer was always filled to set 50 cm^3 constant volumes.

Blending conditions were maintained at 275°C and 80 RPM for 8 min. The following nanoclay (treated and untreated) levels 2,4,5,6 and 8 wt % were used in 70/30/5 wt % PP/PA66/PP-g-MAH blends. The extrudates were palletized before the injection molding. Before a typical mixing operation, the sample mixture was dried overnight at 85°C to minimize hydrolytic degradation of nylons during processing [6].

2.3. Testing

2.3.1 Density Measurement

The density measurement was done using a METTLER TOLEDO high precision balance (10 – 4 g).

2.3.2 Melt Flow Index (MFI)

The Melt Flow Index (MFI) test was performed according to ASTM 1238-85 on a Ray Ran advanced melt flow system machine under a load of 2160 g at 190°C for (PP, PP-g-MAH) and 230°C for the PP/PA66/PP-g-MAH/Nanoclay.

2.3.3 Mechanical Properties

Tensile and impact specimens were prepared according to ASTM D638 and D256 respectively using a Battenfeld injection molding machine.

PP, as well as, PP-PPgMAH-PA66 nanoblends were injection molded under the same conditions: the nozzle temperature was set to be 265°C, the injection pressure was fixed at 75 bar while the screw speed is set to: 70 rpm.

2.3.3.1 Tensile Test

Tensile properties of neat components and the nanoblends were determined at room temperature 23°C according to the procedure described in ASTM D-638 using a computer controlled Zwick DY-25 tensile testing machine operating at 110 mm/min cross-head speed.

Samples were previously dried overnight at 85°C for 24 hours. A total of seven samples were evaluated to obtain average values of the different mechanical properties (stress and elongation at break).

2.3.3.2 Impact Properties

Notched Izod impact strength was determined at room temperature (23°C) according to the procedure described in ASTM D-256 method A. The average specimens dimensions are 63 x 12.7 x 3.17 mm and a notch depth of 2.5 mm. Tests were performed using a ZWICK pendulum apparatus equipped with a 2.7 Joule pendulum. Prior to testing samples were dried overnight at 85°C and allowed to equilibrate at 25°C and 50% humidity for at least 48 hours.

The impact strength was determined as follows:

$$IS = \frac{\theta}{(w - I)xt}$$

Where: IS: Impact strength (KJ/m^2).

W: Width of specimen (m).

I: Notch depth (m).

t: Thickness of specimen (m).

θ: Impact energy (J).
Each data point represents the average value of eight determinations carried out for each formulation.

2.3.4 X-Ray diffraction (XRD) Analysis

Wide-angle X-ray spectra were recorded with a D 500 diffractometer (Philips PW 1710, France) in step scan mode using Ni-filtered CuKα radiation (1.5406 Å). Powder samples (clay) were scanned in reflection, whereas the injection-molded compounds were scanned in transmission in the interval 2 and 70°: The interlayer spacing of the nanoclay was derived from the peak position (d_{001}-reflection) in the XRD diffractograms according to the Bragg's equation.

3. Results and discussion

3.1 MFI

Table 2 represents the variation of MFI versus clay content of both treated and untreated one. It is observed that the MFI values of PP/PA66 nanoblends decreased in the presence of nanoclays. It can be shown that the effect of the treated nanoclay is more pronounced than the untreated one. A drastic reduction in MFI values is observed with a levelling of at 5 wt%. This may be attributed to the interaction between the amine group of the intercalation the nanoclay and anhydride group of the MAH-g-PP. Another possible interaction is between the nanoclay and PA66: the NH_2 group in the octadecylamine is believed to be compatible with PA66 and is capable of forming hydrogen bonds [8]. These interactions reduce the chain mobility and yield lower MFI values.

3.2 Density Measurement

Table.2 represents the variation of densities versus treated and untreated clay content. The effect seems to be minor. Although the densities of the filled nanoblends with treated nanoclay are relatively superior to the untreated ones with a maximum density obtained at 2 wt. %. The treatment seems to lead to a more compact structure. While a decrease is observed with the untreated clay till 5 wt.% is reached followed by an increase.

Table 2
Designation, composition, and MFI and Density values of samples

Sample designation	Composition	Nanoclay content (Phr)	MFI (g/10 min)	Density ρ(g/cm^3)
F0	PP/PA66/PP-g-MAH	0	76,76	0.933
F2	F0/Untreated Nanoclay	2	67,5	0.919
F4	F0/Untreated Nanoclay	4	43,15	0.902
F5	F0/Untreated Nanoclay	5	7,69	0.898
F6	F0/Untreated Nanoclay	6	6,03	0.941
F8	F0/Untreated Nanoclay	8	6,28	0.952
F22	F0/Treated Nanoclay	2	32,41	0.955
F44	F0/Treated Nanoclay	4	8,81	0.926
F55	F0/Treated Nanoclay	5	4,67	0.930
F66	F0/Treated Nanoclay	6	3,72	0.931
F88	F0/Treated Nanoclay	8	3,69	0.950

3.3 Mechanical Properties

3.3.1 Tensile Test

Figure 1 represents the stress at break of PP/PPgMAH/PA66 alloys versus treated and untreated clay content. The systems containing untreated clay show a relatively decreasing stress at break as the clay content increases. In this case, the clay behaves as a filler and due to the lack of interaction with the other components may act as a stress concentrator leading to the observed decrease in stress at break.

In addition to this, some agglomeration may take place as the clay content increases resulting in a reduction of the organoclay aspect ratio, thereby decreasing the contact surface of the organoclay and the matrix polymer.

For the treated clay, a substantial increase in stress at break is observed in the range of 2–4 wt.%, followed by a decrease. A critical clay content seems to be 4wt%. he increase in stress at break originates from interactions between the polymer matrix and the clay through intercalaltion phenomena. For the range of clay content considered, the stress at break of all prepared nanoblends are found to be superior to that of the unfilled formulation. The tensile strength of the nanoblend depends on several factors, such as the dispersion of organoclay inside the matrix, interaction of the clay with the matrix, compatibility between PP and PA66, and the clay-clay interaction. The high aspect ratio of organoclay also enhances the tensile strength of the nanoblend.

Figure 2 depicts the elongation at break of the nanoblends versus treated and untreated clay content A relative steady decrease in elongation at break can be observed as the clay content increases. The effect of treatment is evidenced especially below the critical clay content i.e 4 wt.% where higher elongation at break are observed for the treated clay filled nanoblends. This might be attributed to the good interaction between the clay and the alloy components. Some interaction may have taken place leading to this improvement. Beyond 4 wt.% treated clay, the effect is reversed. Some agglomeration may also have taken place.

3.3.2 Impact Test

Figure.3 represents the notch impact strength of nanoblends versus treated and untreated clay content. About 50% increase in impact strength, when the treated clay is added, is observed. This might be attributed to some intercalation within the clay galleries [10]. Morphological observation seems to support this finding. The flow induced orientation of the clay and the blend component during injection moulding favour this impact strength improvement. 4 wt. % treated clay seems to be a critical concentration. Addition of untreated clay has a minor effect on this property.

3.4 X-ray Diffraction Analysis

Figure 4 (A) and (B) shows the XRD patterns in the range of 2θ = 2–70° for PP-PP-g-MAH-PA66 nanoblends with and without untreated and treated nanoclay respectively. The neat MMT as well as the treated one exhibit a single peak at the low 2θ region at around 2θ = 7.2° and 2θ = 5.9° respectively. It can be observed also that the d_{001} peak shift to lower angles, corresponding to an increase on the basal spacing of the clays by exchange of interlayer spacing with coniums captions. This indicates the ammonium ions intercalate into silicates layers and expand the basal spacing [10].

In fact, the basal spacing increases from 12.18 nm for the neat clay to 15.07 nm for the treated one. Similar observations have been reported elsewhere [11].

The XRD spectra of formulations containing neat clay do not show a characteristic basal reflection of the nanoclay. This is an indication that the clay is just acting as simple filler.

However, formulations containing the treated clay, it can be noticed the disappearance of the characteristic peak of the clay except for formulations F55 and F88. The appearance of two diffuse peaks located close to each other for F55 is explained by partial intercalation as reported in the literature [12].

Concerning formulation F88, the appearance of these peaks could be attributed to the aggregation of small portion clay layers when the clay content is high (8. wt.%). Similar observations have been reported in the literature [13].

Now, as far as the remaining formulations are concerned, the characteristic peak has disappeared suggesting that the gallery distance of the clay in the nanocomposites might be below the resolution of the equipment used in this study [12]. These results indicate also that the PP, PA66 molecular chains may intercalate into the clay galleries and destroy the layer structure of the clay [14].

This is a clear hint that a portion of the nanoclay is only intercalated. The absence of the characteristic clay intense peak in the nanoblends indicates the exfoliation of the clay platelets in the PP matrix. Tang et al [15] attributed the absence of diffraction peaks to the delaminating of the clay. It has been also reported in the literature that the disappearance or decrease of intensity of diffraction peaks could be attributed to the fact that the silicates are partially or completely exfoliated [16, 17].

4. Conclusion

Based on the results of the present study the following conclusions can be drawn. The preparation of PP/PA66/Nanoclay nanocomposite was successful. Addition of treated and untreated nanoclays to the previous blends led to processable blends .i.e., The MFI results revealed a drastic reduction in MFI with a levelling off at 5 wt.% for the nanoblends containing treated clay. The tensile strength and impact properties of PP/PA66 modified nanoblends were improved significantly in the presence of treated nanoclay.

XRD results revealed the formation of nanoblends as the nanoclay was intercalated and exfoliated.

Declarations

Author Contribution

B.K. wrote the main manuscript text and prepared figures . All authors reviewed the manuscript.

References

1. E. M. Araujo, K. D. Araujo, R. A. Paz, T. R. Gouveia, R. Barbosa, E. N. Ito, Polyamide 66/Brazilian Clay Nanocomposites, Journal of Nanomaterials, Vol 2009, 5 pp, (2009).
2. B.N. Ravi Kumar , B. Suresha , M. Venkataramareddy; Effect of particulate fillers on mechanical and abrasive wear behaviour of polyamide 66/polypropylene nanocomposites, Materials and Design, 30, 3852–3858 (2009).
3. Utraki L. A. History of commercial polymer alloys and blends (from a perspective of the patent literature) Polym. Eng. Sci., 35, 2-17 (1995).
4. Yu Z. Z., Yan C., Yang M., Mai Y. W. Mechanical and dynamic mechanical properties of nylon 66/montmorillonite nanocomposites fabricated by melt compounding , Polymer International, 53, 1093-1098 (2004).

5. Heino M.,Kirjava J.,Heitaoja P.,Seppala J.,Compatibilization of Polyethylene Terephthalate/Polypropylene Blends with Styrene-Ethylene/Butylene-Styrene (SEBS) Block Copolymers", J. Appl. Polym. Sci. 65 241-249 (1997).
6. Vocke, C., Anttila, U., Heino, M., Hietaoja, P. & Seppälä J; Use of oxazoline functionalized polyolefins and elastomers as compatibilizers for thermoplastic blends. J. Appl. Polym. Sci., 1998. Vol. 70, s. 1923-1930. (1998).
7. L. Wang et al., Polymer composites-based thermoelectric materials and devices Compos. B Eng. (2017)
8. Kouini B, Combustion behavior of polypropylene/polyamide66/clay nanocomposites,23(1) :68-71 (2016)
9. Huang X. Y., Lewis S., Brittain W. J., Vaia R. A. Synthesis of polycarbonate layered silicate nanocomposites via cyclic oligomers, macromolecules, 33 (2000).
10. Chow W. S., Mohd Ishak Z. A., Karger-Kocsis J., Apostolov A. A., Ishiaku U. S., Compatibilizing effect of maleated polypropylene on the mechanical properties and morphology of injection molded polyamide 6/polypropylene/organoclay nanocomposites, Elsevier Polymer, 44, 7427-7440 (2003).
11. Xie Wei, Gao Zongming, Pan Wei-Ping, Hunter Doug, Singh Anant, Vaia Richard. Chem Mater;13:2979 (2001).
12. D.Garcia-Lopez et al. European Polymer Journal 39 , 945-950 (2003).
13. Vaia RA, Jandt KD,Kramer EJ,Giannelies EP. Kinetics of polymer melt intercalation Macromolecules; 28(24):8080-5 (1995).
14. MA J,Z-N Qi, HU Y. Journal of Applied Polymer Science.82,3611-3617(2001).
15. Tang Yong,Yuan Hu, Polym.Adv.Technol.14,733-737(2003).
16. Nam PH,Maiti P,Okamato M,Kotaka T,Hasegawa N,Usuki A.. Polymer ;42(23):9633-40 (2001).
17. Chengkai Li , Yihan Nie , Haifei Zhan , Jinshuai Bai , Tianshu Liu , Yuantong Gu.Mechanical properties of polymer nanocomposites with randomly dispersed and cross-linked two-dimensional diamond, 230 (1): 109722 (2022).

Figures

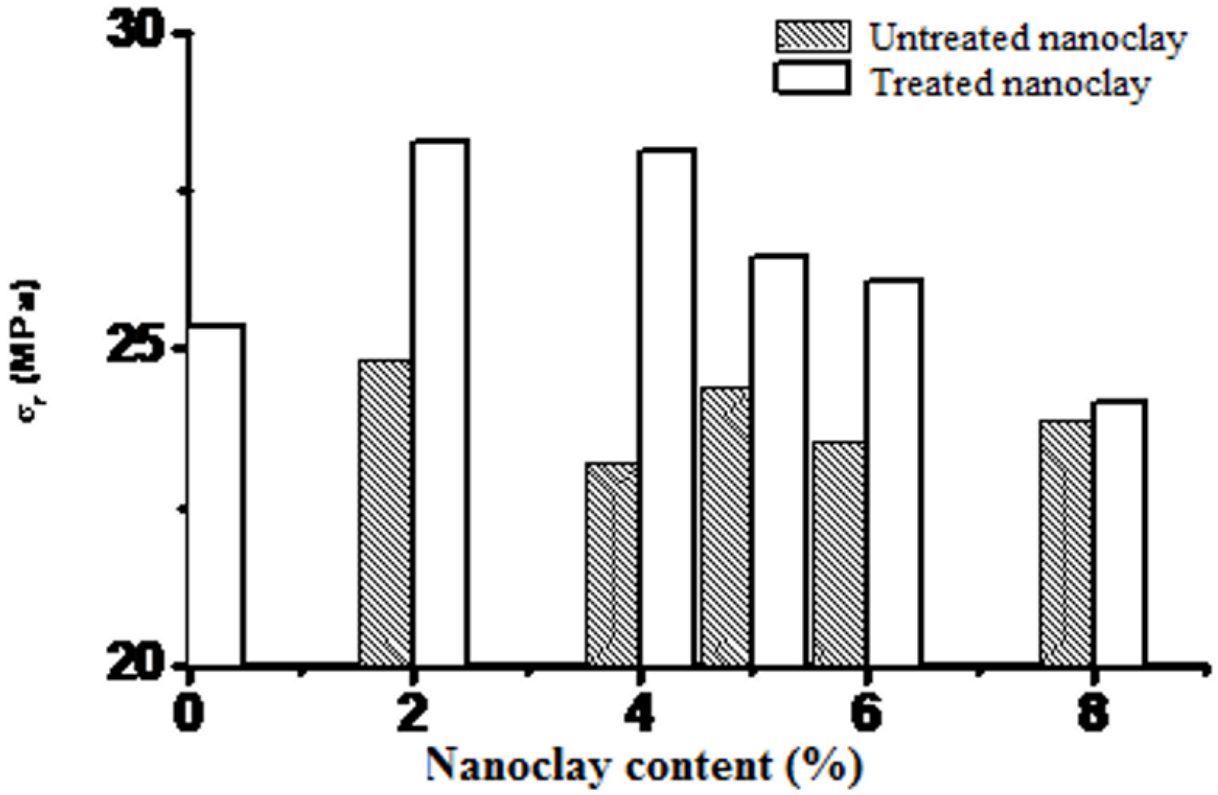


Figure 1

σ_r Vs nanoclay content (%)

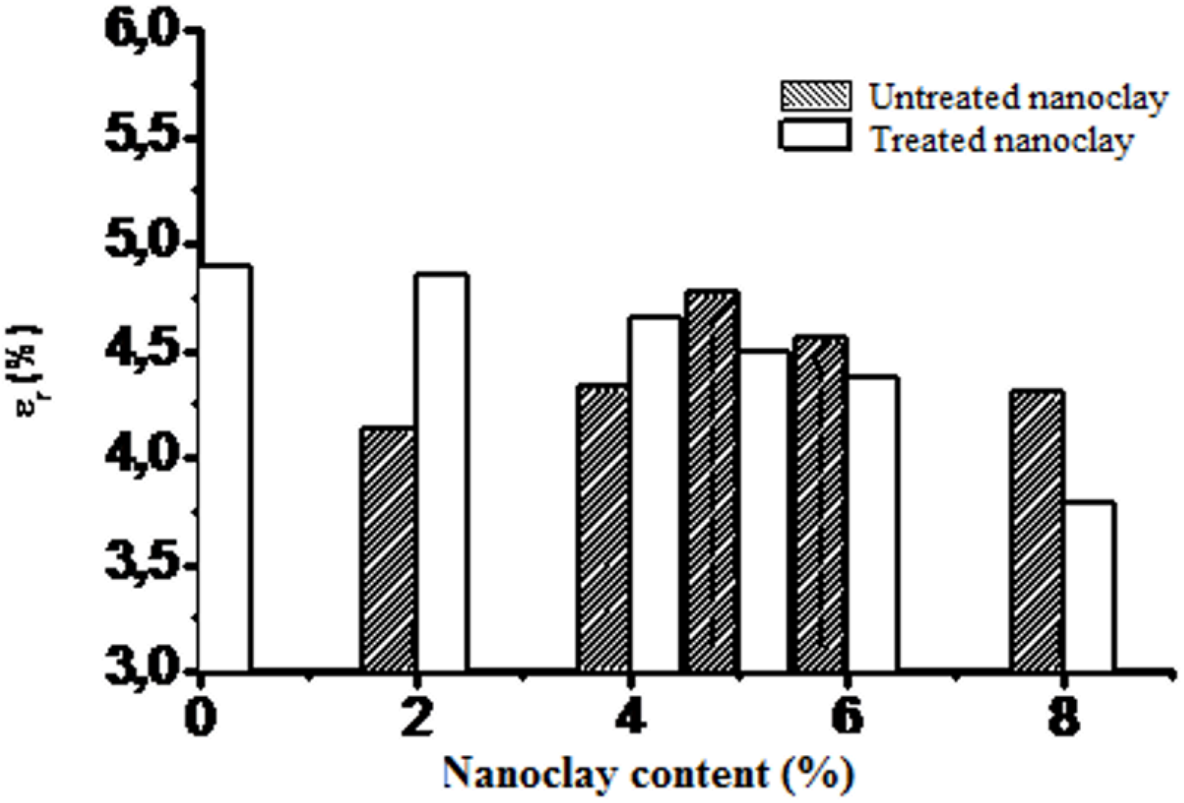


Figure 2

ε_rVs nanoclay content (%)

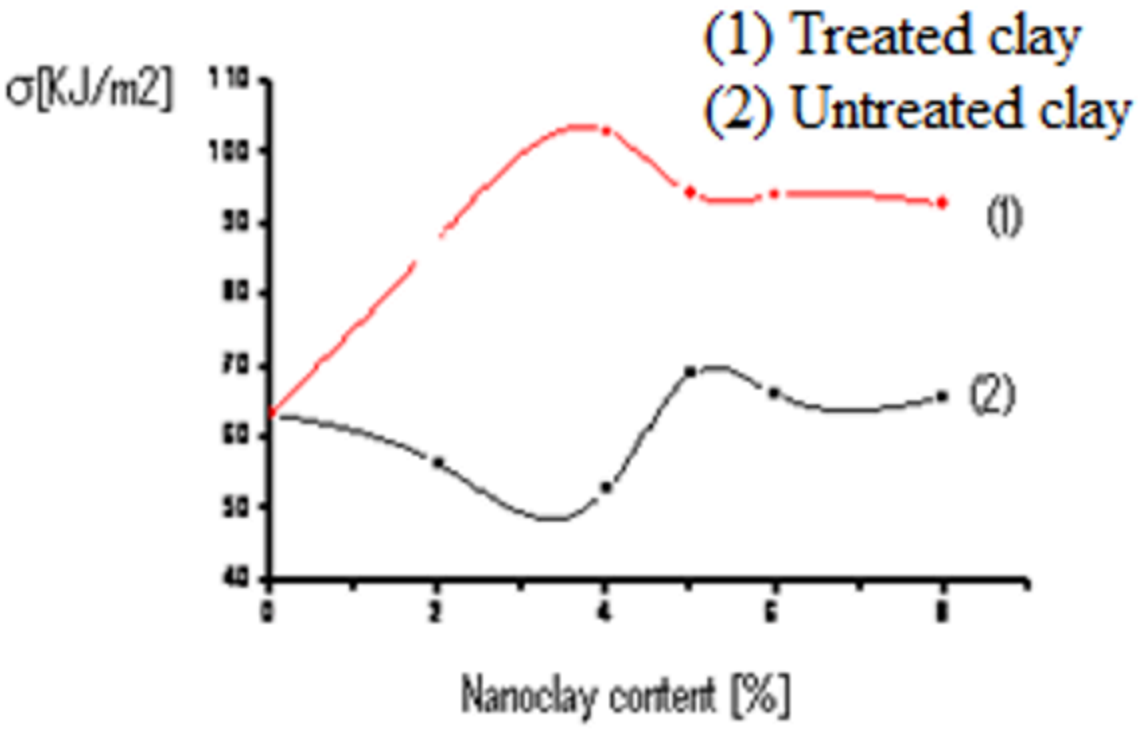


Figure 3

Impact strength vs. nanoclay content

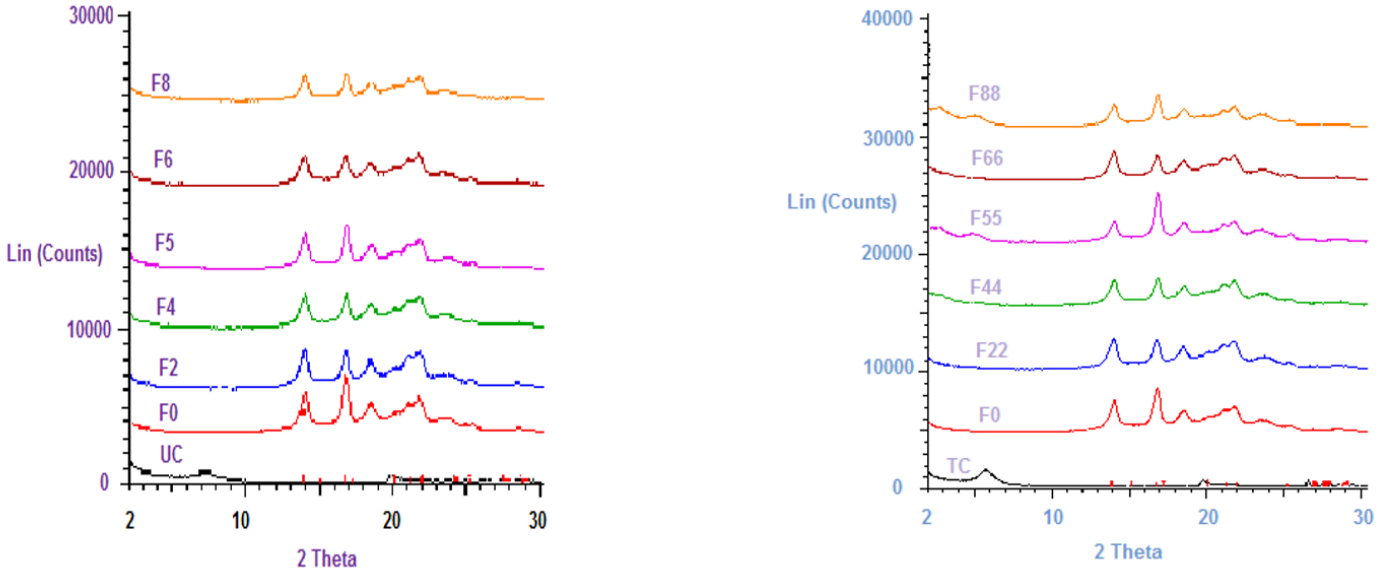


Figure 4

XRD spectra for the neat (A) and modified (B) nanoblends formulations

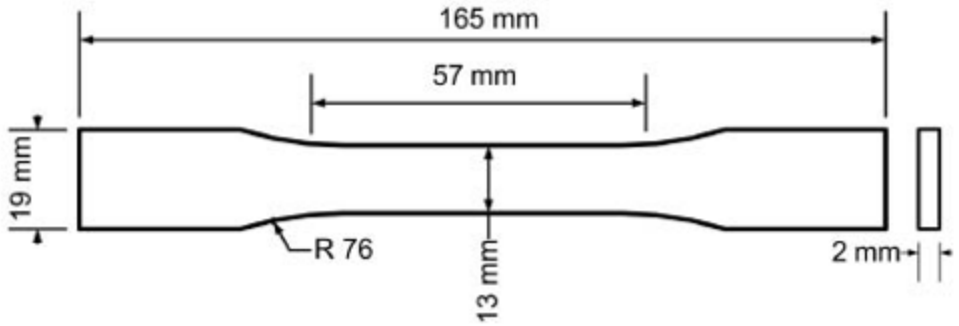


Figure 5

Unnumbered image in the Exprimental section.